Parasitic Array Based Radiation Pattern Reconfigurable Patch Antenna for WLAN Application

Bhaben Saikia and Kunal Borah*

Department of Physics, North Eastern Regional Institute of Science and Technology (Deemed to-be-University), Nirjuli, Itanagar, Arunachal Pradesh, 791109, India.

Corresponding author: Kunal Borah (e-mail: kbnerist@gmail.com).

ABSTRACT This article presents a radiation pattern reconfigurable patch antenna using three rectangular parasitic elements for WLAN (5.8 GHz) application. A rectangular driven patch with two parasitic elements placed parallel to both non-radiating edges and the third parasitic element is located on the radiating edge of driven element. The parasitic elements located on non-radiating edges are loaded with shorting posts. The electrical connection between the post and ground plane is controlled by an RF PIN diode switch. Based on switching state (ON/OFF) of the PIN diodes, post loaded parasitic elements, switch their function between director and reflector to produce beam reconfiguration in the proposed antenna. For different switching combinations of the PIN diodes, beam steering directions in H-plane are obtained at 0˚, +50˚, –50˚ for E-plane radiation maximum at +30˚, while fourth beam steering angle is found at ±50˚ with corresponding E-plane radiation maximum at ±40˚. Measured peak gain of the proposed antenna varies between 3.46 dBi and 3.74 dBi for different beam steering modes. With measured resonant frequency around 5.85 GHz throughout the reconfiguration process, the proposed antenna is considered as a potential candidate for WLAN application.

INDEX TERMS Pattern reconfiguration, Parasitic array, PIN diode, Shorting post, WLAN.

I. INTRODUCTION

Wireless local area network (WLAN) has become a very popular air interface standard for wireless access to telecommunication core network in recent years. As IEEE 802.11 WLAN standard rapidly has become more crowded with users, efficient utilization of allotted frequency bands for this communication standard is very crucial. Reconfigurability in the radiated beam of an antenna contributes on noise avoidance, minimization of co-channel interference and multipath propagation fading by directing signal only towards the desired coverage area. Thus, enhancing the performance of a WLAN system in terms of data security, spectral efficiency and transmission data rate [1–3]. Beam steerable antennas based on phased array technique are usually bulky due to complex phase shifting circuit and power divider unit, which limits their utility for portable wireless devices [4–7]. Implementation of beam steerable antenna with the modified driven patch geometry faces the limitation of variable resonant frequency during beam reconfiguration process [8–10]. Pattern reconfigurable antennas based on Yagi-Uda antenna radiation principle overcome these limitations. These antennas are capable of also steering the direction of maximum radiation at constant resonant frequency with compact antenna dimension [11–13]. The parasitic elements in these antennas act as switchable director or reflector.

In [14], a beam steerable antenna with a 3 × 3 parasitic pixel layer above the driven patch is investigated for 2.4 GHz WLAN application. Twelve RF PIN diode switches are employed between the adjacent pixels to change the parasitic pixel geometry. This in turn, produces beam steering along nine different directions in the semisphere space ($\theta \in \{-30˚, 0˚, 30˚\}$; $\Phi \in \{0˚, 45˚, 90˚, 135˚\}$). The antenna employs large number of PIN diodes along with a DC biasing circuitry consisting large number of inductors and capacitors, which increases its complexity. An antenna with pattern reconfigurability for WLAN and WiMAX application is reported in [15]. Two parasitic stubs along with four ideal switches in the ground plane perform the function of reflector to switch the H-plane radiation pattern from omnidirectional to a directional mode. A beam steerable active superstrate antenna is presented in [16] for 5.25 GHz WLAN application. Eight RF PIN diodes are

inserted at bottom side of the superstrate which produce a phase delay of the radiated fields for beam tilting at +11° and –23°. A beam steerable patch antenna with parasitic pixel layer for 2.45 GHz WLAN band is reported in [17]. The pixel layer contains 31 hexagonal copper pieces and zero-ohm chip resistors are used to form pixel groups. Activation of different pixel groupings produce beam steering at tilt angles +15° and –15°. Another pattern reconfigurable antenna for 2.45 GHz WLAN application is presented in [18]. A driven circular monopole patch is surrounded by three ship-shaped parasitic patches at the top face while two parallel metal strips at the bottom of the antenna. Beam steering in +30° and –30° directions is reported with the help of two PIN diodes associated with the metal strips. In [19], a parasitic array beam steerable antenna based on two embedded PIN diode is discussed with resonant frequency 5.8 GHz for all tilt angles, dedicated for WLAN application. The embedded PIN diodes act as shorting post upon activation and steer the main lobe at +30°, 0° and –30° directions for different switching combinations.

In this article, a pattern reconfigurable parasitic array antenna based on switchable shorting posts is proposed for 5.85 GHz WLAN application. This antenna steers its beam into four different directions corresponding to four switching combinations of two PIN diodes associated with the shorting posts. PIN diodes and all components of DC biasing circuitry are mounted on the ground plane to minimize possible disturbances in the radiated fields of the antenna. Unlike the beam steerable antennas reported for WLAN application in [15–19] which are able to reconfigure their radiation pattern either in H-plane or E-plane, pattern reconfiguration in both planes (E and H) are achieved in the proposed antenna. Enhancement of beam steering capability in terms of beam tilt angle and steering direction is the additional advantage of the proposed pattern reconfigurable patch antenna (PRPA).

II. ANTENNA GEOMETRY DESIGN AND PATTERN RECONFIGURATION PRINCIPLE

The proposed PRPA consists of a rectangular driven patch and three parasitic elements, which is designed and fabricated on a FR4 substrate (ε_r = 4.4) of dimension (45 × 65 × 1.6) mm^3. As illustrated in Fig. 1, parasitic element 1 (PE1) and parasitic element 2 (PE2) are placed near both non-radiating edges of the driven patch. The parasitic element 3(PE3) is positioned at the radiating edge opposite to feed line. Size of the driven patch is calculated for 5.8 GHz using transmission line model (TLM) of patch antenna

[20] and found as length L_p = 11.75 mm and width W_p = 15.74 mm. The driven patch is fed with a microstrip line of length l_f = 17 mm and width w_f = 0.8 mm while impedance matching over 5.8 GHz WLAN band is achieved with an inset of optimal size x = 3 mm and y = 1.3 mm. Ansoft High Frequency Structure Simulator (HFSS) ver. 13.0 is used for determining the optimal size of parasitic elements to achieve maximum possible tilt angle and are found as length L = 11.87 mm, width W = 15.90 mm. To reconfigure the parasitic elements between reflector and director, two shorting posts namely post 1 and post 2 of radius 0.7 mm are inserted at inimitable positions (u_1, v_1) and (u_2, v_2) of PE1 and PE2 respectively. As shorting post location is crucial in the beam steering process of parasitic array, they are optimized for maximum tilt angles. Two RF PIN diodes PD1 and PD2 are mounted on rectangular slots of the ground plane. These PIN diodes control the function of shorting posts by establishing electrical connection between parasitic patches and ground plane. Length and width of these rectangular slots are 7 mm and 6.5 mm respectively.
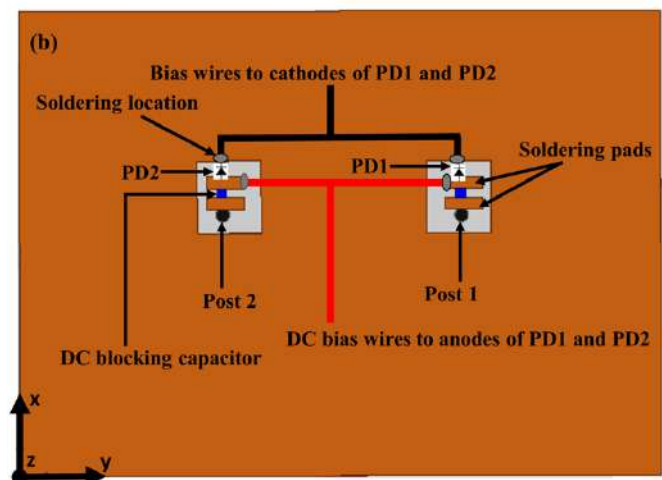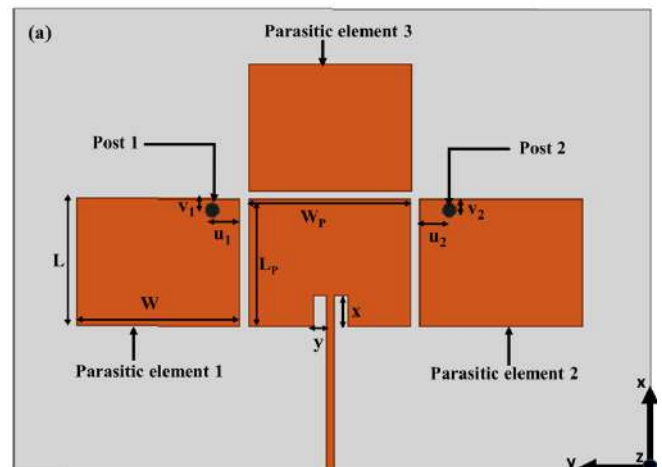
For ON state operation of a PIN diode, positive DC voltage is applied at its anode with the bias wire soldered at metallic pad, while the wires soldered at ground plane serve as bias lines to PIN diode cathode. DC bias circuit for each PIN diode employs a 10 pF DC block capacitor, which is mounted between the soldering pads as shown in the Fig. 1(b). PIN diode switches and associated DC bias circuitry are designed at bottom face in the proposed PRPA to lower the possibility of any interference with radiated field. Optimal values of different design parameters are listed in Table I.

TABLE I. Optimal values of design parameters

Driven patch	L_p = 11.75 mm	W_p = 15.74 mm
Parasitic element	L = 11.87 mm	W = 15.90 mm
Inset dimension	x = 3 mm	y = 1.3 mm
Position of shorting post 1	u_1 = 2.8 mm	v_1 = 1.14 mm
Position of shorting post 2	u_2 = 3 mm	v_2 = 1.14 mm

A. PATTERN RECONFIGURATION PRINCIPLE

When a parasitic element is placed adjacent to a driven patch, electromagnetic coupling induces a current in the element. The distribution of this induced current determines the radiation characteristics such as gain and main lobe orientation of the array. In the proposed antenna, two shorting posts and ON-OFF switching of RF PIN diode associated with each shorting post alters the induced current distribution along with effective electrical length of these elements. This causes the elements to perform their function either as reflector or director for beam steering which is identical to the radiation mechanism of Yagi-Uda antenna [21]. For ON state operation of a PIN diode, the induced current flows from the parasitic element to the ground plane through the shorting post. This increases the electrical length of the element and the element functions as a reflector. In contrast, OFF state operation of PIN diode causes the element to act as director, since the induced current does not flow through the shorting post to reach the ground plane.

For different switching combinations of PIN diodes PD1 and PD2, four beam steering modes are obtained in the proposed PRPA. For mode 1 operation, only PD1 is turned ON which configures the PE1 as reflector while PE2 as director and deflects the H-plane main lobe towards right (+50˚). In mode 2, PD2 is turned ON while PD1 switched

to OFF state for reconfiguration of PE1 as director and PE2 as reflector. This, in turn, steers the main lobe in opposite direction of tilting as obtained in mode 1 (–50˚). Both PD1 and PD2 are operated in OFF state for mode 3 operation, and H-plane radiation pattern is directed towards the broadside direction (0˚). In mode 1, mode 2 and mode 3 operation, E-plane beam maximum remains constant (+30˚). For mode 4 operation, PD1 and PD2 are turned ON which produces a bidirectional radiation pattern in H-plane (±50˚) along with beam reconfiguration in E-plane (±40˚).

B. ANTENNA DESIGN EVOLUTION

1) INITIAL ANTENNA GEOMETRY

Unlike the final antenna geometry as shown in Fig. 1, initial antenna structure contains only two parasitic patches namely, PE1 and PE2 on a FR4 substrate of size (35 × 65 × 1.6) mm³ which is illustrated in Fig. 2. Optimal values of all other design parameters are same as those presented in Table 1.
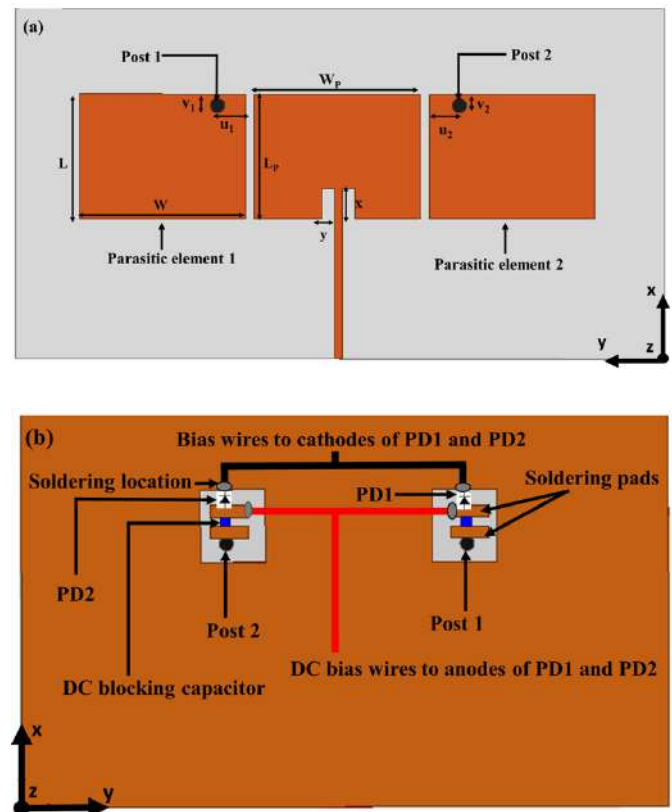

FIGURE 2. (a) Top, and (b) Bottom view of initial antenna geometry.

From HFSS simulation, it is found that this parasitic antenna structure steers the H-plane beam maximum at +45˚, –45˚, 0˚ and ±50˚ for different switching

combinations of PD1 and PD2. Direction of E-plane beam maximum is fixed at –15° throughout the reconfiguration process. Simulation results of reflection coefficient S_{11}, E and H-plane radiation pattern for all beam steerable modes are illustrated in Fig. 3.
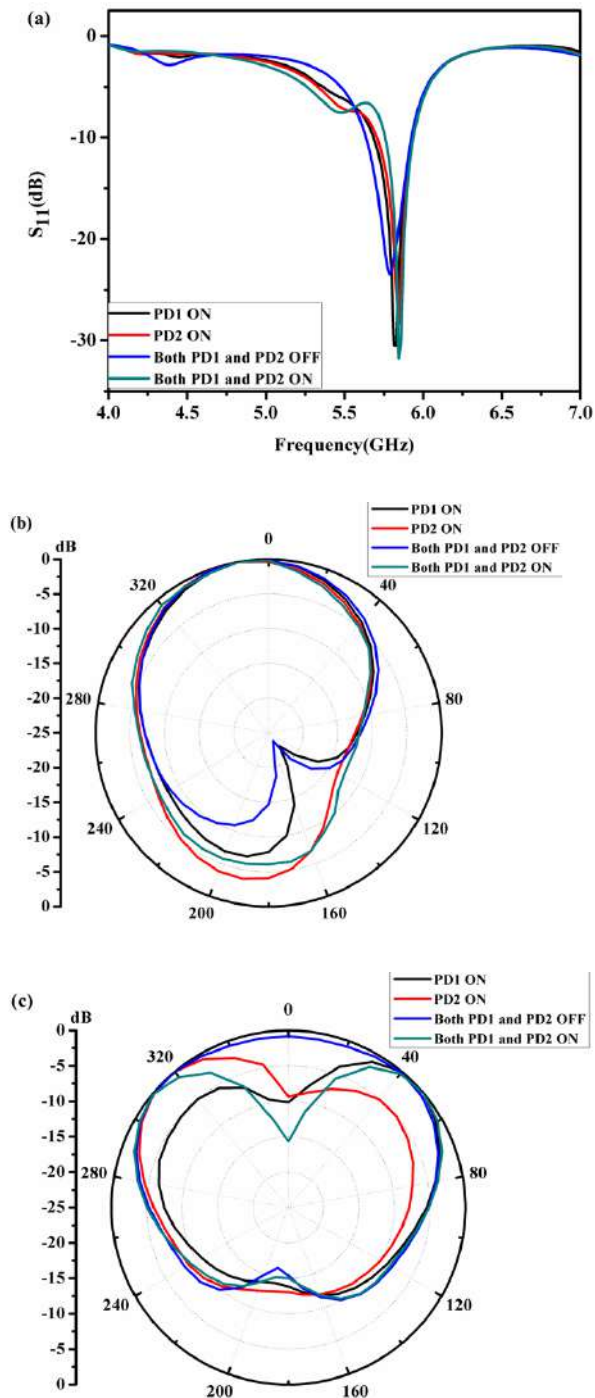

FIGURE 3. (a) Reflection coefficient, (b) E plane, and (c) H plane radiation pattern of initial antenna geometry for different modes.

From S_{11} plot, it can be seen that resonant frequency of this antenna is around 5.8 GHz with acceptable return loss for all tilt angles. However, significant side lobes/back lobes are observed in the radiation pattern plots, which contributes to poor directivity and small average gain of 2.12 dB in the antenna. Moreover, E-plane beam reconfiguration is not achieved in the antenna.

2) FINAL ANTENNA GEOMETRY

To improve the gain and directivity of the antenna discussed in section 2.2.1, parasitic element 3 is placed at the radiating edge of driven patch as shown in Fig. 1. However, no shorting post is introduced in PE3 to limit the use of PIN diodes and other biasing circuit components. The final antenna structure is able to steer the H-plane radiation maximum at 0°, +50°, –50° and ±50° while E-plane radiation pattern reconfigured at +30° and ±40°. Thus, improvement in front to back ratio along with enhancement in tilt angle and peak realized gain is achieved in the final antenna.

SMP 1345-040LF PIN diode from Skyworks Solutions is employed in the proposed antenna. This PIN diode is primarily chosen because of extremely small size, low forward resistance (1.5 Ω) and small reverse capacitance (0.15 pF). In simulation, the PIN diode is modeled as RLC equivalent circuit. In ON state it is equivalent to series combination of an inductance $L_s = 0.45$ nH and resistance $R_s = 1.5$ Ω. For OFF state operation, it is modeled with an inductance $L_s = 0.45$ nH which is in series with a parallel grouping of OFF state resistance 5 kΩ and reverse capacitance $C_p = 0.15$ pF.

C. PARAMETRIC STUDY

Spacing between the driven and parasitic element, size of parasitic element should be optimized for enhanced beam tilt angle and reflection coefficient S_{11}, which is carried out with HFSS by tuning one parameter at a time while keeping another parameter constant. This optimization is done for mode 1 operation and is kept same for other modes.

1) EFFECT OF DRIVEN AND PARASITIC ELEMENT SPACING

Electromagnetic coupling is considered as an important factor for beam steering in the proposed PRPA, which depends on the spacing s between the active and parasitic element. Effect of s on S_{11} and radiation pattern, for different values of s can be seen in Fig. 4. As s is decreased from 1.4 mm to 0.6 mm by step size of 0.2 mm, S_{11}

improves from –16.9 dB to –34.5 dB with a corresponding change in resonant frequency from 5.78 GHz to 5.87 GHz. E-plane beam maximum remains 30° throughout the variation process of s, however side and back lobes decrease gradually for decremental change in s and becomes minimum at $s = 0.8$ mm. For $s = 0.6$ mm, side and back lobe again increases.

From H-plane pattern plot, it can be seen that beam tilt angle is 40° for $s = 1.4$ mm, 1.2 mm while it is 50° for $s = 1$ mm, 0.8 mm, 0.6 mm values. However, at $s = 0.8$ mm, proposed PRPA offers optimum front to back ratio and directivity. As tilt angle and directivity are the most desirable performance parameters in this antenna, hence $s = 0.8$ mm is considered as the optimal value.

2) EFFECT OF PARASITIC ELEMENT LENGTH

The effect of parasitic element length L on reflection coefficient and beam tilt angle are also investigated by changing L as $1.02 \times L_P$, $1.01 \times L_P$, L_P and $0.98 \times L_P$. As shown in the Fig. 5, simulated S_{11} values are –20.1 dB (5.81 GHz), –26 dB (5.83 GHz), –32.2 dB (5.86 GHz) and –23.02 dB (5.84 GHz) for L = $1.02 \times L_P$, $1.01 \times L_P$, L_P and $0.98 \times L_P$ respectively. From E-plane radiation pattern plot, it can be seen that direction of beam maximum is at 40° for L = $1.02 \times L_P$, and remains constant at 30° for L = $1.01 \times L_P$, L_P and $0.98 \times L_P$. Again, beam tilt angle is obtained as 50° in H-plane for all L values used in the parametric study. However, L = $1.01 \times L_P$ is considered as the optimal parasitic length because of superior radiation characteristics in terms of directivity, front to back ratio and gain.
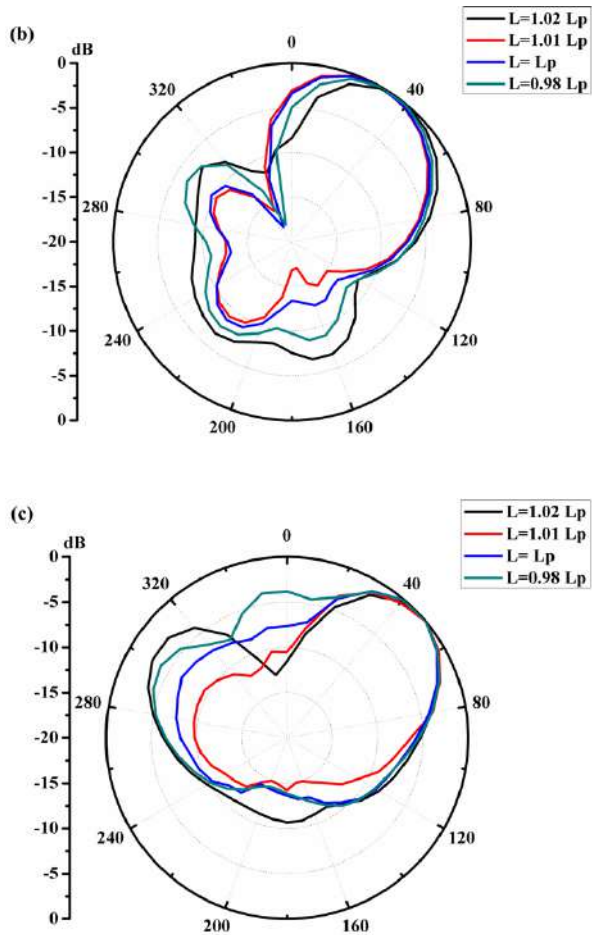

(a)

(b)

(c)

(a)
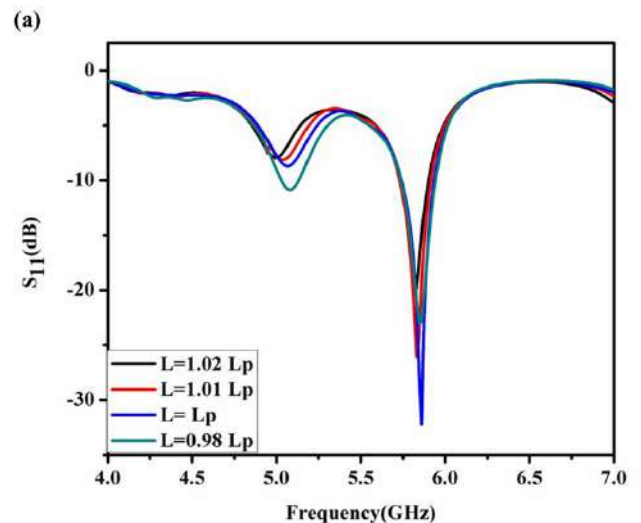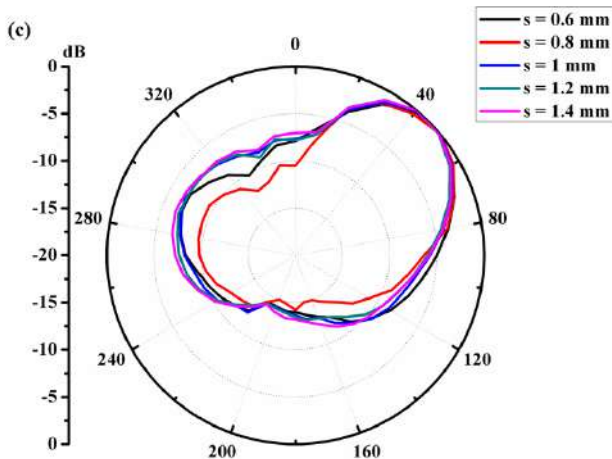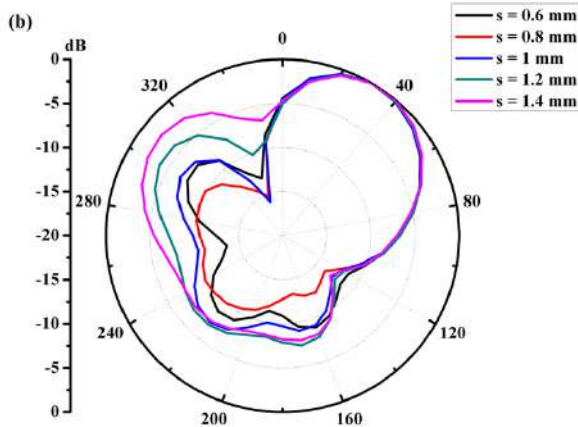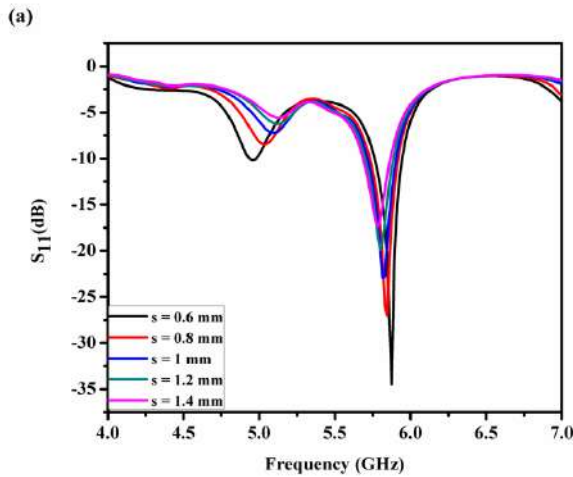
FIGURE 5. (a) S_{11}, (b) E plane, and (c) H plane radiation pattern, for different values of L.

III.   RESULTS AND DISCUSSION

To validate the design theory and simulation results, final antenna geometry is fabricated as shown in the Fig. 6, and the return loss S_{11} and radiation pattern of the fabricated antenna for different beam steering modes are measured using Agilent N5247A vector network analyzer (VNA) and Anechoic chamber measurement set-up respectively. VNA is calibrated using Thru-Reflect-Line (TRL) technique with a 3.5 SMA calibration kit.

A.   RETURN LOSS S_{11} MEASUREMENT

For different switching combinations of PIN diodes PD1 and PD2, the proposed PRPA can be operated in four operating modes for reconfiguration in radiation pattern. Measured resonant frequencies for mode 1, mode 2, mode 3 and mode 4 are obtained at 5.87 GHz, 5.83 GHz, 5.90 GHz and 5.95 GHz while corresponding simulated values are

observed at 5.83 GHz, 5.84 GHz, 5.83 GHz and 5.86 GHz respectively, as illustrated in Fig. 7.
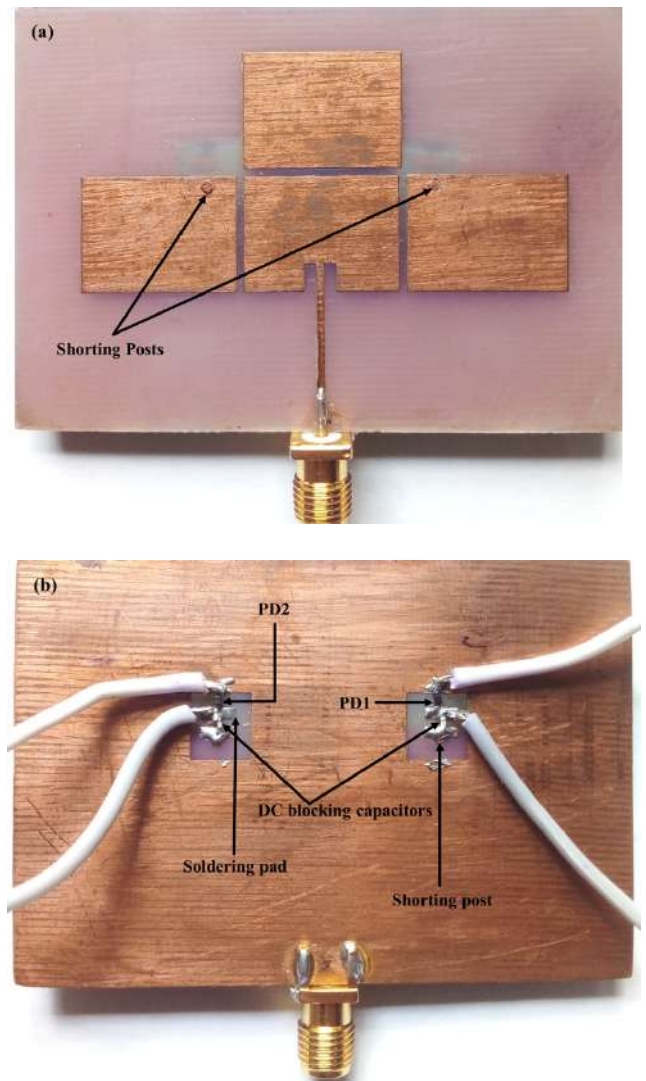
FIGURE 6. Fabricated antenna (a) Top, (b) Back side.

It can also be seen that measured resonant frequencies cover 5.68 GHz—6.05 GHz frequency bandwidth centred at 5.85 GHz, which is assigned for WLAN application. Simulation and measurement results of resonant frequency, S_{11} and % bandwidth for various operating modes is compared in Table II. Small variation can be observed between the simulated and measured values of S_{11} and –10 dB percentage bandwidth, which could be attributed to the fabrication tolerances and presence of DC bias wires.

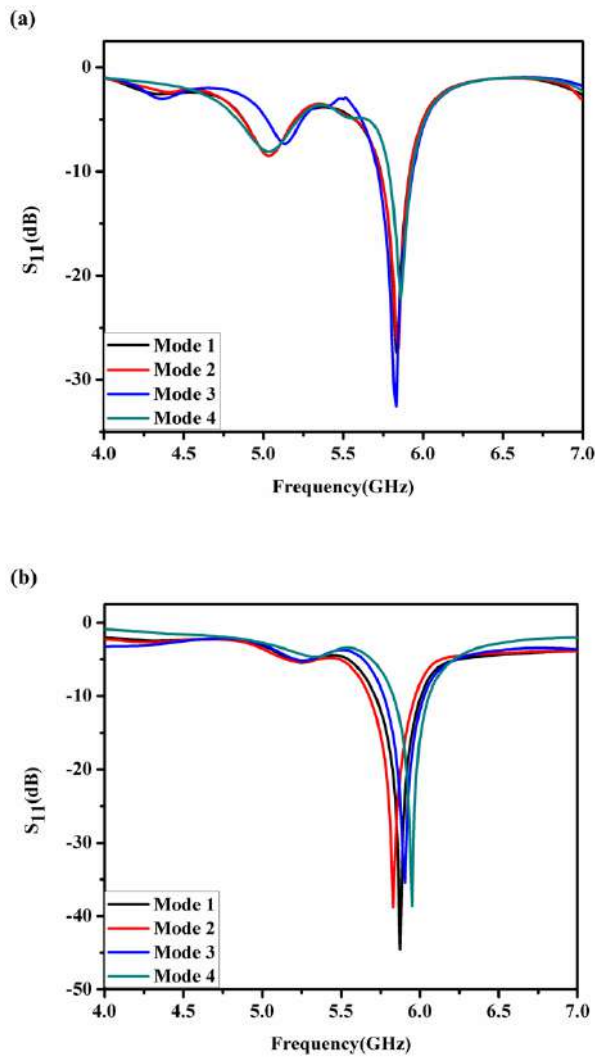**FIGURE 7.** (a) Simulated, and (b) Measured S_{11} plot for different modes of the proposed PRPA.

TABLE II. Comparison of simulated and measured resonant frequency, S_{11} and −10 dB percentage bandwidth.

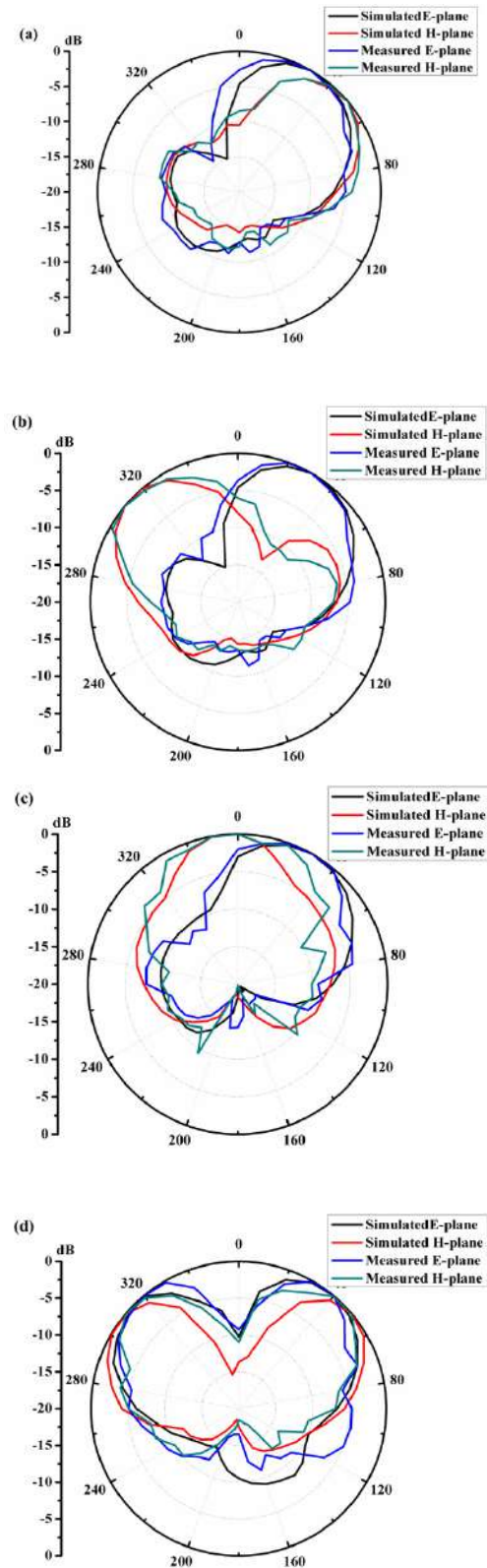| Modes of operation	Resonant frequency (GHz)		S_{11} (dB)		−10 dB % bandwidth	
	Sim.	Meas.	Sim.	Meas.	Sim.	Meas.
Mode 1	5.83	5.87	−27.3	−44.5	3.09%	4.93%
Mode 2	5.84	5.83	−26.9	−38.8	3.25%	4.97%
Mode 3	5.83	5.90	−32.6	−35.4	3.77%	4.24%
Mode 4	5.86	5.95	−22.1	−38.6	2.56%	3.69%

FIGURE 8. E and H plane radiation pattern (a) Mode 1, (b) Mode 2, (c) Mode 3 and (d) Mode 4.

B. RADIATION PATTERN AND GAIN MEASUREMENT

The E and H-plane radiation pattern of the fabricated antenna is measured in an anechoic chamber measurement set-up for all operating modes and is depicted in Fig. 8.

TABLE III. Simulated and measured results of beam tilt angle and antenna gain for various reconfiguration modes.

Modes	Tilt angle				Antenna Gain (dBi)	
	Sim.		Meas.		Sim.	Meas.
	E	H	E	H		
Mode 1	+30˚	+50˚	+30˚	+50˚	4.18	3.74
Mode 2	+30˚	−50˚	+30˚	−50˚	4.15	3.71
Mode 3	+30˚	0˚	+30˚	0˚	4.08	3.46
Mode 4	±50˚	±50˚	±40˚	±50˚	3.99	3.49

From the comparative plot of normalized radiation pattern illustrated in Fig. 8, it can be observed that measured radiation pattern of the fabricated antenna is identical to the simulated pattern and offers beam tilt angles in H plane at +50˚, –50˚ and 0˚, for E plane beam maximum at 30˚ in mode 1, mode 2 and mode 3 operation respectively. In mode 4 operation, bidirectional H plane pattern is obtained at tilt angle ±50˚ with respective E plane beam maximum at ±40˚.

Conventional two antenna method is adopted for gain measurement of the fabricated antenna and average peak gain of 3.6 dBi is obtained. It is observed that the average value of measured gain varies by 0.5 dBi compared to the simulated values. Losses arises in actual SMD components (PIN diodes and capacitors) can lead to such variations in gain [19]. A comparison of simulation and measurement results of beam tilt angle and antenna gain are listed in Table III.

A comparison of the proposed PRPA in terms of design and performance parameters with other relevant works is presented in Table IV.

TABLE IV. Comparison of the proposed PRPA with other relevant works   (λ_0 = free space wavelength at lowest resonant frequency).

Ref. No.	Overall Size (λ_0^2)	Switch type and Quantity		DC bias circuitry	Peak gain (dBi)	Beam tilt angles	Operating Band
[15]	0.32 × 0.32	Metallic strip	4	Not required	3.2	Omnidirectional, +90˚, –90˚ (H- plane)	WLAN (2.4, 5.2, 5.8 GHz), WiMAX (3.5,5.5 GHz)
[16]	1.58 × 1.58	PIN diode	8	Not present	12.8	+11˚, –23˚	WLAN (5.25 GHz)
[17]	Not reported	Chip resistor	24	Not required	5.704	+15˚, –15˚	WLAN (2.45 GHz)
[18]	0.29 × 0.20	PIN diode	2	Present	0.77	+30˚, –30˚ (H- plane)	WLAN (2.45 GHz)
[19]	0.62 × 1.47	PIN diode	2	Present	6.5	0˚, +30˚, –30˚ (H plane)	WLAN (5.8 GHz)
[22]	0.72 × 1.13	PIN diode	4	Present	4.7	0˚, +40˚, –40˚, ±45˚ (H plane)	Wi-Fi 6E (5.925–6.425 GHz
This work	0.88 × 1.27	PIN diode	2	Present	3.6	+50˚, –50˚, 0˚, ±50˚ (H plane), +30˚, ±40˚ (E plane)	WLAN (5.85 GHz)

IV. CONCLUSION

A parasitic array based PRPA with embedded shorting posts and PIN diodes is reported in this article. The PIN diodes associated with the shorting posts control the current flow in the parasitic array. The conducting states of the PIN diodes helps in altering the effective electric length of the parasitic elements which eventually act either as reflector or director for beam steering purpose. Parametric studies reveal that, the gap between driven and parasitic element, and the size of parasitic elements have significant effect on beam tilt angle and gain of beam steerable parasitic array. The proposed antenna can reconfigure the H plane radiation pattern in four distinct configurations and E plane pattern in two directions around 5.85 GHz resonant frequency, thus fulfilling diverse requirements of WLAN application.

REFERENCES

[1] W. S. Kang, J. A. Park, and Y. J. Yoon, "Simple reconfigurable antenna with radiation pattern," *Electronics Letters*, vol. 44, no. 3, pp.182-183, 2008.

[2] A. G. Besoli, and F. D. Flaviis, "A multifunctional reconfigurable pixeled antenna using MEMS technology on printed circuit board," *IEEE Transactions on Antennas and Propagation*, vol. 59, no. 12, pp.4413–4424, 2011.

[3] I. Ben Trad, J. M. Floc'H, H. Rmili, M. Drissi, and F. Choubani, "A planar reconfigurable radiation pattern dipole antenna with reflectors and directors for wireless communication applications," *International Journal of Antennas and Propagation*, vol. 2014, pp.1-10, 2014.

[4] S. K. Sanyal, Q. M. Alfred, and T. Chakravarty, "A novel beam- switching algorithm for programmable phased array antenna," *Progress In Electromagnetics Research*, vol. 60, pp.187-196, 2006.

[5] G. Exposito Dominguez, J. M. Fernández González, P. Padilla de La Torre, and M. Sierra Castañer, "Dual circular polarized steering antenna for satellite communications in X band," *Progress In Electromagnetics Research*, vol. 122, pp.61-76, 2012.

[6] T. Yuan, N. Yuan, J. L. W. Li, and M. S. Leong, "Design and analysis of phased antenna array with low sidelobe by fast algorithm," *Progress In Electromagnetics Research*, vol. 87, pp.131-147, 2008.

[7] F. Mubasher, S. H. Wang, X. D. Chen, and Z. Ying, "Study of reconfigurable antennas for MIMO systems," *Proceedings of the 2010 International Workshop on Antenna Technology (iWAT'10), IEEE,* pp.1-4, 2010.

[8] C. Won Jung, M. J. Lee, G. P. Li, and F. D. Flaviis, "Reconfigurable scan-beam single-arm spiral antenna integrated with RF-MEMS switches," *IEEE Transactions on Antennas and Propagation*, vol. 54, no. 2, pp.455-463, 2006.

[9] J. Sarrazin, Y. Mahé, S. Avrillon, and S. Toutain, "Pattern reconfigurable cubic antenna," *IEEE Transactions on Antennas and Propagation*, vol. 57, no. 2, pp.310-317, 2009.

[10] S. Nikolaou, R. Bairavasubramanian, C. Lugo, I. Carrasquillo, D. C. Thompson, G. E. Ponchak, J. Papapolymerou, and M. M. Tentzeris, "Pattern and frequency reconfigurable annular slot antenna using PIN diodes," *IEEE Transactions on Antennas and Propagation*, vol. 54, no. 2, pp.439-448, 2006.

[11] X. Yang, B. Wang, S. Yeung, Q. Xue, and K. Man, "Circularly Polarized Reconfigurable Crossed-Yagi Patch Antenna," *IEEE Antennas and Propagation Magazine*, vol. 53, no. 5, pp.65-80, 2011.

[12] S. Zhang, G. Huff, J. Feng, and J. Bernhard, "A Pattern Reconfigurable Microstrip Parasitic Array," *IEEE Transactions on Antennas and Propagation,* vol. 52, no. 10, pp.2773-2776, 2004.

[13] Z. Shi, R. Zheng, J. Ding, and C. Guo, "A novel pattern-reconfigurable antenna using switched printed elements," *IEEE Antennas and Wireless Propagation Letters*, vol. 11, pp.1100-1103, 2012.

[14] Z. Li, E. Ahmed, A. M. Eltawil, and B. A. Cetiner, "A beam-steering reconfigurable antenna for WLAN applications," *IEEE Transactions on Antennas and Propagation*, vol. 63, no. 1, pp.24-32, 2014.

[15] S. Koley, L. Murmu, and B. Pal, "A pattern reconfigurable antenna for WLAN and WiMAX systems," *Progress In Electromagnetics Research C*, vol. 66, pp.183-190, 2016.

[16] N. Shoaib, S. Ilyas, A. Raza, and T. Hassan, "Beam steering using active superstrate antenna for WLAN applications," *IEEE International Symposium on Antennas and Propagation and USNC-URSI Radio Science Meeting*, IEEE, pp.2029-2030, July, 2019.

[17] K. Yilmaz, and T. Nesimoglu, "Design of a multi-layer beam-steering WLAN antenna," *18th Mediterranean Microwave Symposium (MMS)*, IEEE, pp.26-31, November, 2018.

[18] X. He, P. Gao, Z. Zhu, S. You, and P. Wang, "A flexible pattern reconfigurable antenna for WLAN wireless systems," *Journal of Electromagnetic Waves and Applications*, vol. 33, no. 6, pp.782-793, 2019.

[19] T. Sabapathy, M. F. B. Jamlos, R. B. Ahmad, M. Jusoh, M. I. Jais, and M. R. Kamarudin, "Electronically reconfigurable beam steering antenna using embedded RF PIN based parasitic arrays (ERPPA)," *Progress In Electromagnetics Research*, vol. 140, pp.241-261, 2013.

[20] C. A. Balanis, "Antenna theory: analysis and design," 3rd ed., John wiley & sons, 2015, pp. 816-826.

[21] J. Huang, and A. C. Densmore, "Microstrip Yagi array antenna for mobile satellite vehicle application," *IEEE Transactions on Antennas and Propagation*, vol. 39, no. 7, pp.1024-1030, 1991.

[22] B. Saikia, and K. Borah, "A Parasitic Array Based Pattern Reconfigurable Patch Antenna for Wi-Fi 6E Application," *Progress In Electromagnetics Research M*, vol. 107, pp.119-129, 2022.